Photovoltaic Energy Harvesting with Static and Dynamic Solar Modules Employing IoT-Enabled Performance Monitoring

Krismadinata Krismadinata [1], Asnil Asnil [1], Irma Husnaini [1], Remon Lapisa [1], Ricky Maulana [1], Muldi Yuhendri [1], Erita Astrid [2], Premalatha Logamani [3]

[1]*Centre for Energy and Power Electronics Research (CEPER), Universitas Negeri Padang, Indonesia*
[2]*Department of Electrical Engineering, Universitas Negeri Medan, Indonesia*
[3]*School of Electrical Engineering, Vellore Institute of Technology, Chennai, India*

*Abstract –*This study examines the effectiveness of static and dynamic PV module models for solar energy gathering. The static design of the first solar panel is used, while the dynamic design of the second solar panel with a single-axis tracker is used. Finding the best model for capturing solar energy and turning it into electrical energy is the aim. Monitoring systems use IoT technologies. To detect variables including current, voltage, radiation, temperature, and humidity, the system has a number of sensors. The Thinger i.o program, coupled to the Arduino Uno used to control these sensors uses the Internet of Things (IoT) concept to evaluate and keep track of the outcomes of parameter measurements. As a result, the acquired measurement results can be viewed on the Thinger i.o application and checked remotely from any location. The three tests show that systems using dynamic ideas are better able to capture solar energy than static systems. The performance discrepancy is at its widest in the third test, when the dynamic system generates 14.4% more electrical energy than the static system.

*Keywords –*Energy harvesting, solar modules, single-axis solar tracker, IoT.

1. Introduction

Renewable energy is a key priority due to rising demand for electricity, the global energy crisis, environmental degradation, fossil fuel pricing, and climate change [1], [2]. Solar energy, which is abundant, limitless, and ecologically friendly, is becoming more popular [3], [4]. Despite high investment costs and limited conversion efficiency [5], [6]. Thus, increasing solar energy conversion efficiency to electrical energy is always a fascinating subject [7], [8].

Solar panels can be made more efficient by tracking the sun [9], [10], [11], [12]. It generates the maximum energy when its surface is perpendicular to the sun. In other words, solar panels absorb exactly the same quantity of solar radiation as they create energy [13], [14]. However, the sun's position, which fluctuates from morning to evening, cloud shadows on the solar panel, and ambient temperature are the key issues. This sun position tracker directs the solar panel's surface toward the strongest incoming sunlight. Therefore, solar panel systems that track the sun create more electrical energy [15], [16].

Methods for tracking can be broken down into categories such as movement type, controller, and number of degrees of freedom. Different types of motion call for different strategies for keeping tabs on the sun's location. Passive solar trackers rely on a liquid substance whose motion is controlled by the difference in liquid density generated by a temperature difference, rather than electronic components [16]. However, the effectiveness of this type is greatly diminished by its reliance on climatic factors. In contrast, an active solar tracker uses a microprocessor for automated operation, a computer and time for data control, and sensors to mechanically adjust the solar panel's surface to face the sun at different times of day [17].

The sun-tracking angle is shown in Figure 1 [18] depicts the angle of movement for tracking the position of the sun, which is classified into two types.

The first is the zenith, also known as the elevation angle, which is the sun tracker's movement from north to south. While azimuth is the movement of the sun's tracker position from east to west. The sun moves approximately 150 degrees per day and 46 degrees north to south each year first is the zenith, or elevation angle, which is the sun tracker's north-south movement. The sun's tracker location moves east to west in azimuth. Each year, the sun moves 46 degrees from north to south and 150 degrees per day [19]. Every day, the earth receives approximately 1300 watts of power per hour per meter [20].
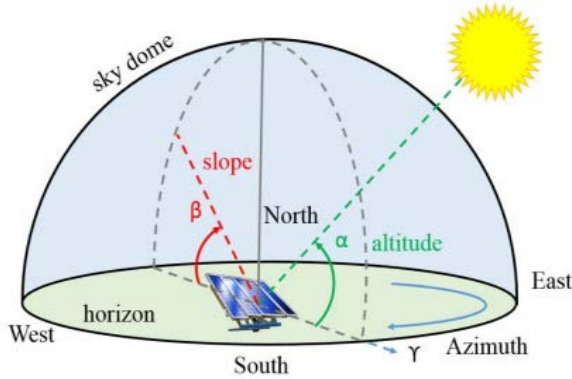

Figure 1. Sun position tracking angle [18]

This paper explains tracking the sun's location with a single axis using Thinger.io, an IoT-based application that displays electrical parameters. Compared to systems that don't employ the sun position tracker principle, this single-axis tracker is cheaper, simpler, and more efficient. This research aims to absorb the most solar radiation and transform it into electricity using solar panels. By placing the solar panel's surface perpendicular to the sunlight, it converts solar energy into electrical energy more efficiently.

2. Tracking System Movement

The energy resulted from a PV system is largely determined by location, global horizontal irradiation (GHI), direct normal irradiation (DNI), ambient temperature conditions, components used in the PV system (cables, inverters, transformers, etc.) [21]. Determining the relative sun's position is very important to calculate the sun's irradiation on the surface, which in known as the zenith, azimuth, angle of incident and tracking angle. The peak of the sun $((\theta_z)$(zenith)) is the existing angle between the line of observation to the sun and the line perpendicular to the horizontal plane.

The angle that exists between the north and the projection line of the sun's plane on a horizontal surface is known as azimuth (γ_s). Meanwhile, the angle of incidence is the angle between the normal line to the surface of the module and the sunlight.

Equation (1), (2), and (3) can be used to determine the zenith, azimuth, and angle of incidence values for a single axis tracker [21], [22].

$$\theta_z = \arccos(\sin\varphi\sin\delta + \cos\varphi\cos\delta\cos\omega) \quad (1)$$

$$\gamma_s = arcsin\left(\frac{\cos\delta\sin\omega}{\cos\theta_z}\right) \quad (2)$$

$$\theta_i = \arccos(\cos\theta_z * \cos\beta\cos(\gamma_s - \gamma) * \sin\theta_z.sin\beta) \quad (3)$$

Where (φ) is the latitude, (δ) is the declination angle, (ω) is the hour angle), (γ) is the azimuth angle of the surface and (β) is the tracking angle. If the value $(\gamma_s \leq 0^0)$ then the surface of the solar panel will face the east, so that the value $(\gamma = -90^0)$ while the value is $(\gamma_s > 0^0)$ then the surface of the solar panel will face the west so that the value is $(\gamma = 90^0)$. The tracking angle is between -900 (northern earth) and 900 (southern earth), which is the angle between the soil layer and the tracking surface, which can be described in equation (4).

$$\beta = arctan\left(\frac{sin(\gamma_s - 180)}{tan(90 - \theta_z)}\right) \quad (4)$$

3. Prototype Design and Implementation

This research is conducted to determine how to convert solar energy into electrical energy using a single axis solar tracking system. The design and construction of this system can be divided into three parts: the physical design of the solar module drive structure, the control system, and the monitoring system

3.1. The Prototype Design

The prototype design of solar tracking system can be seen in Figure 2. The mechanical structure for solar module propulsion is designed to operate as efficiently as possible. The constructed structure can only move from east to west. This structure is propelled using a linear actuator, and the movement is determined by the difference in the intensity of the sun that is measured by two LDRs. The specifications of the solar modules can be found in Table 1.

Figure 2. The constructed tracking system

Table 1. The solar module specifications

Product specifications	
Type of module	SP-20-P36
Rated power (Pmax)	20 W
Current at Pmax (Imp)	1.15 A
Voltage at Pmax (Vmp)	17.4 V
Short-circuit current (Isc)	1.23 A
Open circuit voltage (Voc)	22.4 A
Number of cells	36

3.2. Control System

Figure 3 depicts the control system's diagram for the sun position tracking system using this single axis. The mechanical drive, which directs the surface of the solar module from east to west in accordance with the sun's movement, employs a linear actuator model BHTGA 300-12-5. The actuator moves based on the difference in sunlight intensity, which is obtained by using two Light Dependent Resistors (LDR) that are processed using an Arduino Uno. Meanwhile, several sensors are used to obtain the desired parameters such as ACS712, F031-06, BH1750, and DHT11 to measure current, voltage, solar radiation, temperature, and humidity, respectively. Then, the obtained parameters from each sensor are processed using an Arduino Uno and then displayed on an IoT platform application as a monitoring system. A NodeMCU 8266 processor serves as a transmitter to transmit data from the system to the IoT platform (Thinger i.o) through a wireless network.

From Figure 3, it can be seen that the solar module control consist of several elements such as solar module, solar charger, battery, buck converter, arduino uno, relay, NodeMCu 8266, LDR, voltage sensor, current sensor, BH1750, DHT11, actuator as a mechanical drive for solar modules. In addition, the energy generated by solar modules is stored in batteries and also can be used as a source for the system's operation.
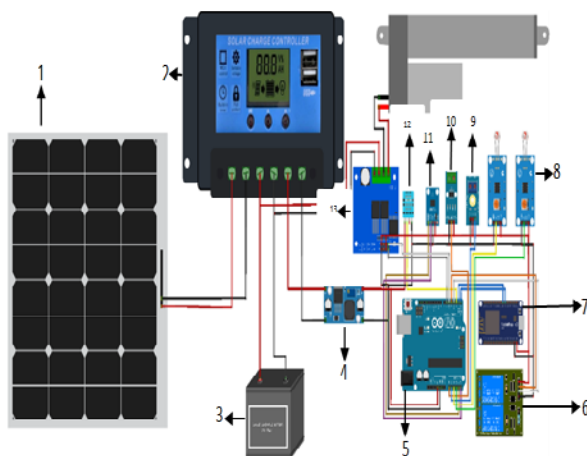
3.3. Monitoring System

A monitoring system is designed to monitor the solar module parameters such as current, voltage, the sunlight intensity, temperature, and humidity and it is illusrated in the Figure 4.
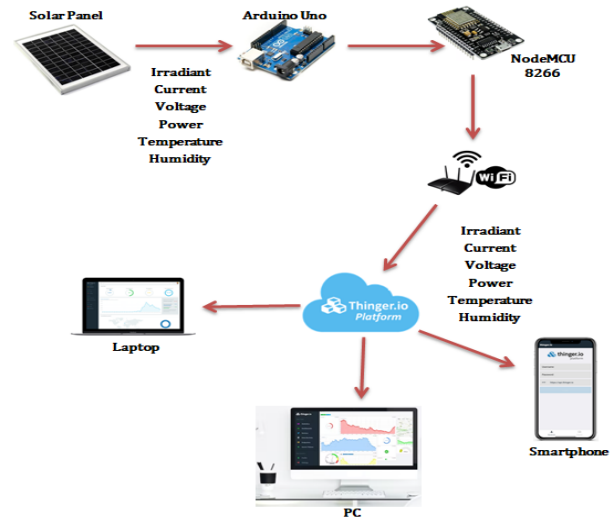

Figure 4. The monitoring diagram using IoT

Using sensors, all necessary parameters are gathered and transmitted to Arduino Uno. They are then forwarded from Arduino Uno to NodeMCu 8266 as a transmitter for transmission to the Thinger i.o (IoT platform). The transmission process from the NodeMCU 8266 to the Thinger i.o uses a wireless network intermediary. The data in Thinger i.o is accessible via computer, notebook computer, or mobile device. Users can access data in the Thinger i.o application from any location and at any time as long as they and the system are connected to the Internet. Furthermore, the algorithm describing how the system works is presented in Figure 5.
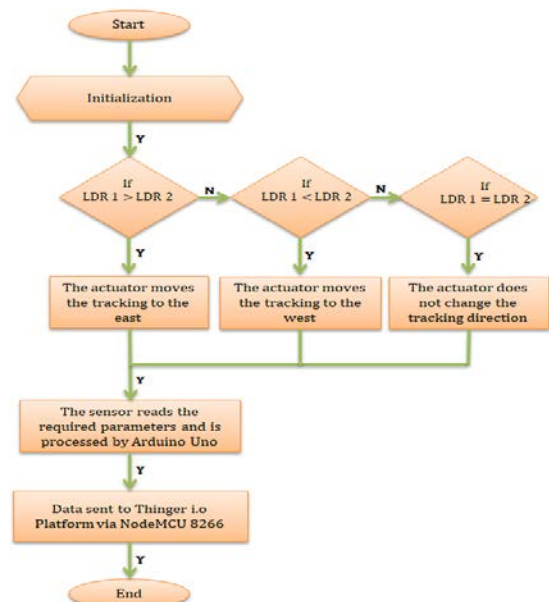

Figure 3. The control diagram of the solar module system.

Figure 5. Algorithm for monitoring

4. Results and Discussion

Figure 6 illustrates a built-solar module system with a single-axis solar tracking (dynamic) system and fixed (static) system. To observe its effectiveness in harvesting solar energy, a test is conducted and the results are compared to those of a fixed system. The system is evaluated under a variety of environmental conditions, including variations in temperature, solar radiation, and the effect of shading from morning to afternoon. The test results are then recorded and displayed on the Thinger i.o platform.

Figure 6. The Experiment test setup

Figure 7 depicts a comparison of voltage outputs from solar module systems with fixed and tracking systems.
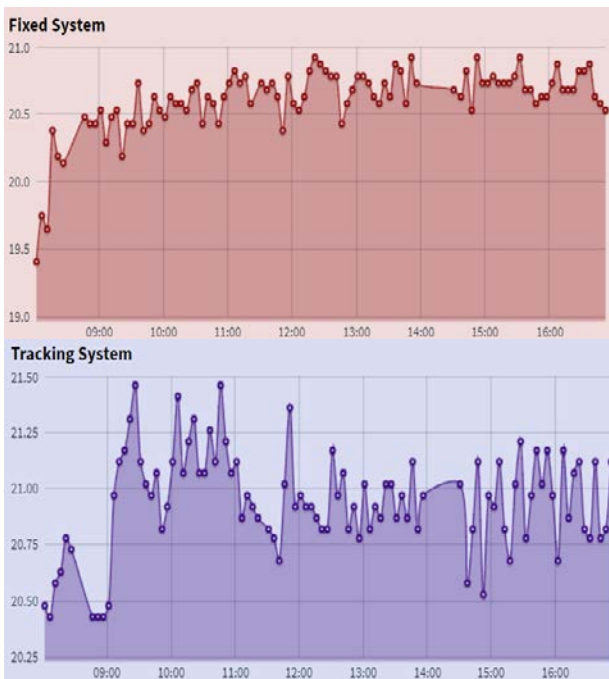

Figure 7. The open circuit voltage measurements

During the test, the voltage values change based on the weather conditions.

In systems that do not employ the concept of tracking, the voltage values tend to rise from the beginning of the test until 9:00 a.m. Then these values remain stable with slight fluctuations around 20.5 volts. In contrast, the voltage values in tracking-based systems vary significantly from the beginning to the end of the test.
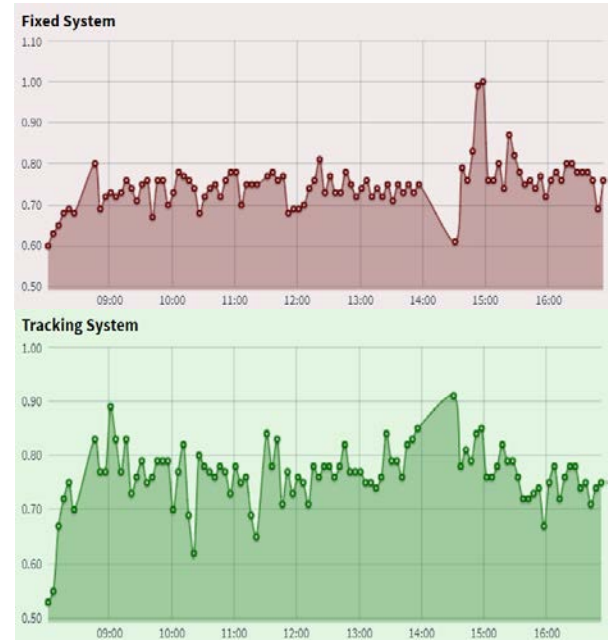

Figure 8. The short-circuit measurements

Figure 8 illustrates the current outputs of solar module systems from fixed and tracking systems. Both systems have considerably fluctuated currents due to the influence of weather conditions that cause differences in solar radiation reaching the surface of the solar module. In general, the current values generated by the two systems tested are still above 0.7 amperes.

The generated power during the test follows the pattern of the generated voltage and current can be shown in Figure 9. The data are compared accordingly.

The characteristics of humidity, temperature, and solar radiation during the test are depicted in Figure 10. The characteristics of humidity and temperature are clearly opposite. If the temperature rises, the humidity level will fall, and vice versa. From the beginning of the test until 9 a.m., the solar radiation reaching the surface of the solar modules tends to increase.

This condition occurs due to cloudy weather in the morning, which prevents sunlight from reaching the surface of the solar module. The intensity of the sunlight then reaches a stable condition before gradually increasing after 2 p.m. However, starting at 3 p.m., the solar radiation dramatically decreased and changed eccentrically until the test concluded.
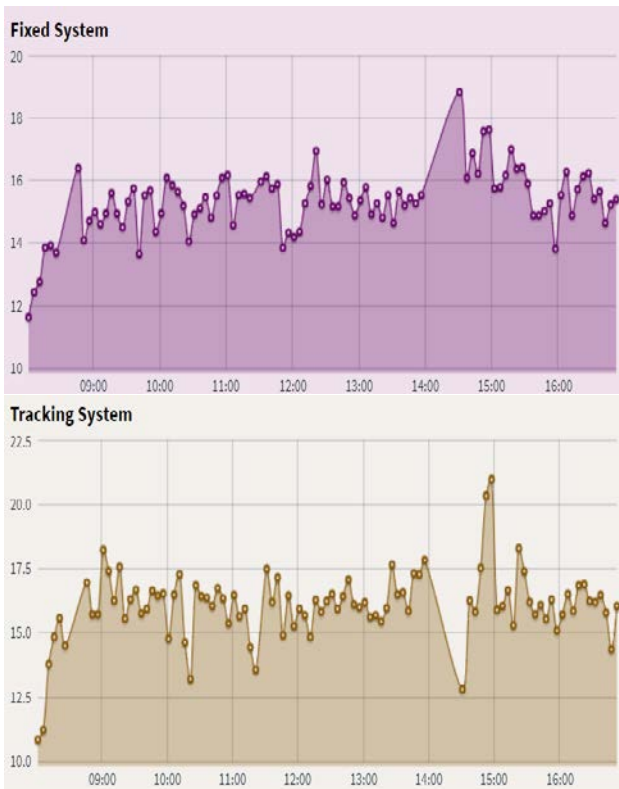
Figure 9. The generated power

Figure 10. The environmental data at the time of measurement namely: humidity, temperature, irradiance

This is due to the fact that after 03:30 p.m. more clouds cover the sun, preventing the sunlight from reaching the surface of the solar modules.

The first day of testing takes place in cloudy conditions from the start until around 9 a.m. However, the weather remains sunny until around 15.00, when clouds begin to influence the weather until the test is completed. The average electrical energy generated by a fixed system is 14.50 W, while a tracking system generates 15.24 W. The values of all measured parameters for every hour during the test from 8 a.m. to 5 p.m. are presented in Tables 2 to 4.

The comparison of voltage, current, and generated power by two solar tracker systems involving the fixed and tracking systems on the first day of testing are also presented in the graphs shown in Figures 11, 12, and 13, respectively.

In general, the voltage generated by a system employing the tracking concept is greater than the output of a fixed system. Similarly, there are fluctuations in the resultant current value, but the tracking-based system still produces a greater value. Moreover, the electric energy produced is proportional to the magnitude of the test's current value. Figure 13 demonstrates that the system employing the tracking concept produces more energy than the fixed system.
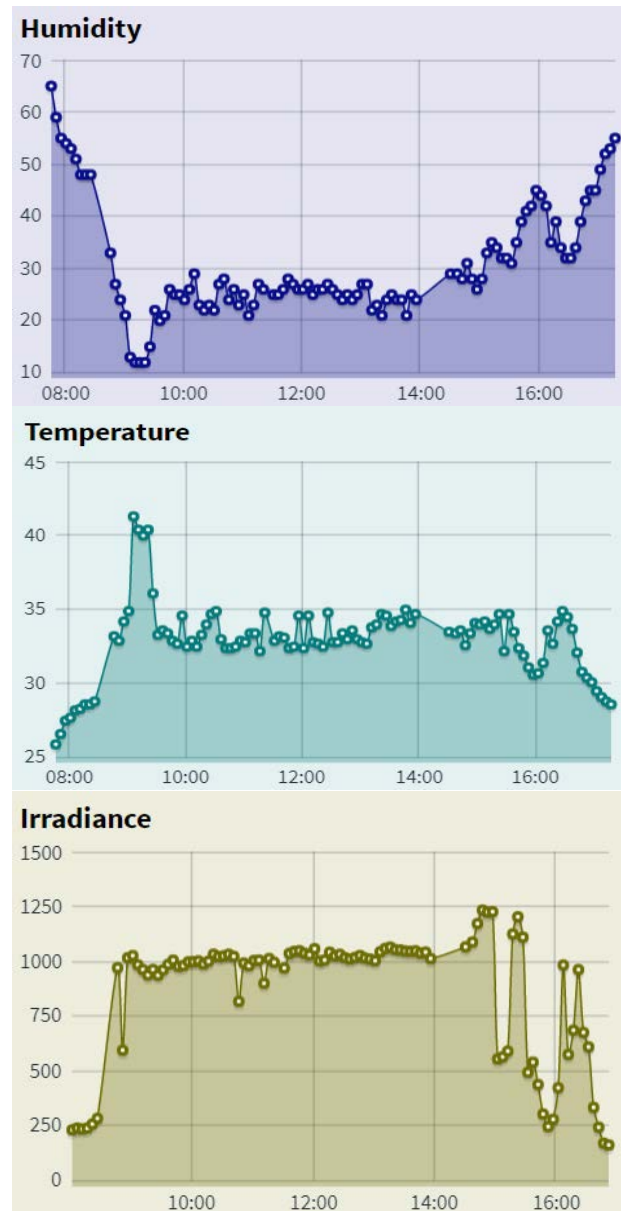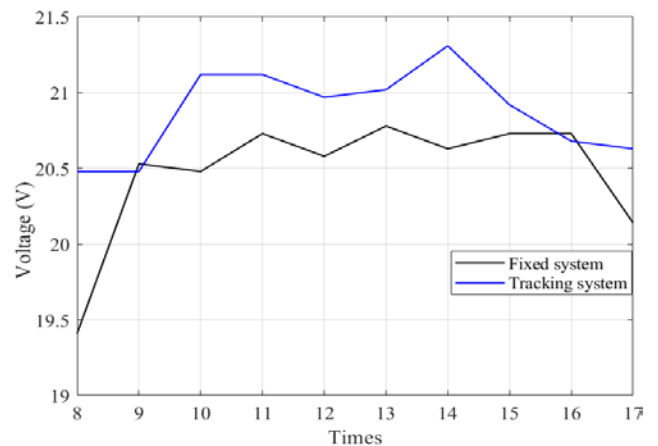

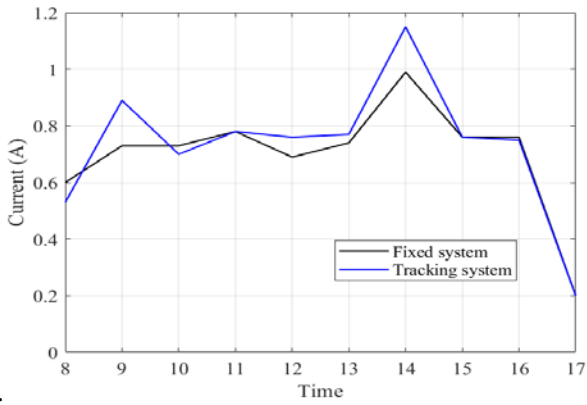*Figure 11. The comparison of open-circuit voltage*

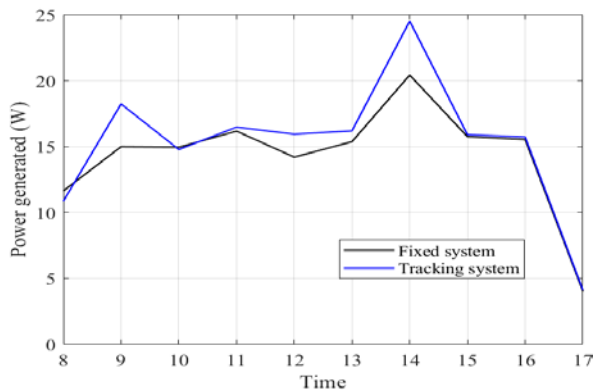Figure 12. *The comparison of short-circuit currents*

Figure 13. *The comparison of the power generated*

On the second day, the test is conducted in sunny weather but it is interspersed with clouds, particularly after 3 p.m. until the test ended. The test results are illustrated in Figures 14, 15, and 16 for voltage, current, and energy as outputs from the fixed and tracking systems. In general, the solar tracking system generates a greater amount of power than the fixed system does. It can be seen in Figure 14 that the voltage outputs of both systems vary and fluctuate. However, the voltages in the fixed system drop significantly after 3 p.m. In terms of current values, either a solar tracking system or a fixed system has fluctuating currents until these values tend to decrease at the end of the test. There are fluctuations in the resultant current value, but the tracking-based system still produces greater values as illustrated in Figure 15. Moreover, the electrical energy generated from both systems on the second day of testing as shown in Figure 16 also experienced a drastic decrease in the afternoon until the testing was completed. This is due to a significant number of clouds in the sky during the test, which prevents sunlight from reaching the surface of the solar module.

Table 2. *Test parameter value every hour during the test on first day*

Time	Voltage (V)		Current (A)		Power (W)		Temperature (^{0}C)	Humidity (%)	Irradiance (W/m^2)
	Fixed system	Tracking system	Fixed system	Tracking system	Fixed system	Tracking system			
08.00	19.41	20.48	0.60	0.53	11.64	10.86	27.70	54.00	232.96
09.00	20.53	20.48	0.73	0.89	14.69	18.23	34.90	21.00	1026.34
10.00	20.48	21.12	0.73	0.70	14.95	14.78	32.50	24.00	999.17
11.00	20.73	21.12	0.78	0.78	16.17	16.47	32.80	25.00	1004.17
12.00	20.58	20.97	0.69	0.76	14.20	15.94	32.40	26.00	1057.74
13.00	20.78	21.02	0.74	0.77	15.37	16.19	32.80	27.00	1003.15
14.00	20.63	21.31	0.99	1.15	20.42	24.51	33.80	27.00	973.28
15.00	20.73	20.92	0.76	0.76	15.75	15.90	34.00	28.00	556.24
16.00	20.73	20.68	0.76	0.75	15.54	15.72	30.70	44.00	424.70
17.00	20.14	20.63	0.20	0.20	4.03	4.13	29.50	49.00	54.97

Table 3. *Test parameter value every hour during the test on second day*

| Time	Voltage (V)		Current (A)		Power (W)		Temperature (^{0}C)	Humidity (%)	Irradiance (W/m^2)
	Fixed system	Tracking system	Fixed system	Tracking system	Fixed system	Tracking system			
08.00	20.97	20.38	1.07	1.03	22.44	21.00	29.50	40.00	288.33
09.00	20.92	20.63	1.07	1.22	22.39	25.17	34.30	19.00	871.10
10.00	20.78	20.82	1.00	1.15	20.78	23.95	34.40	30.00	803.36
11.00	20.92	20.82	1.13	1.05	23.64	21.87	33.60	26.00	1043.66
12.00	21.07	21.07	1.05	1.18	22.12	24.80	34.40	29.00	651.80
13.00	21.17	20.82	0.93	1.19	19.68	24.78	32.30	36.00	591.77
14.00	20.97	21.07	1.13	1.03	23.70	21.70	33.80	25.00	1032.47
15.00	21.07	20.97	1.04	0.95	21.91	19.92	29.30	48.00	496.59
16.00	20.29	20.34	0.50	0.41	10.14	8.34	26.00	66.00	126.80
17.00	20.58	19.70	0.25	0.33	5.15	6.50	27.20	56.00	5.19
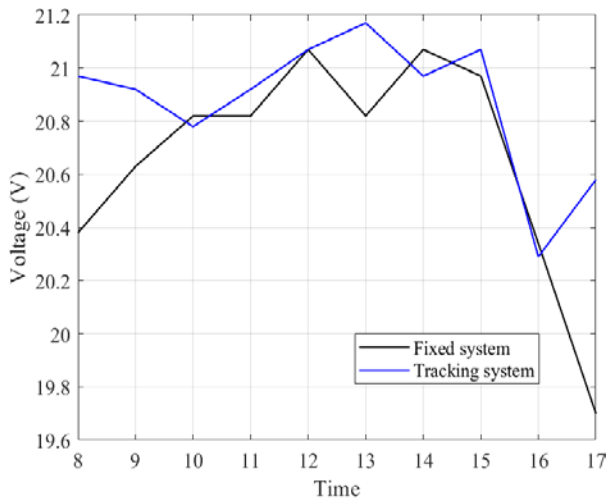
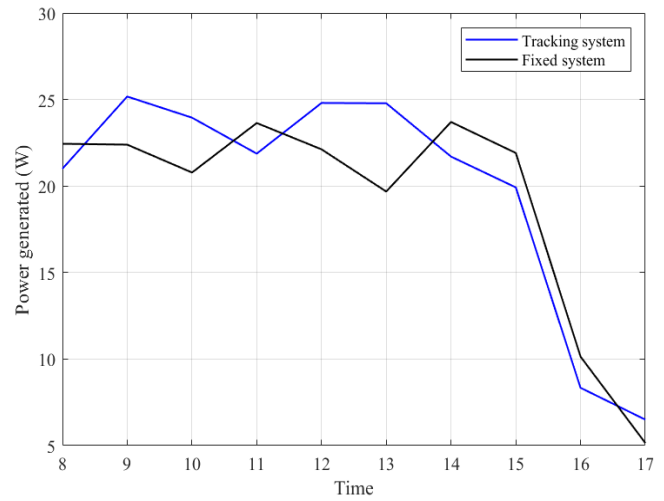*Figure 14. The open-circuit voltages on the 2nd day*
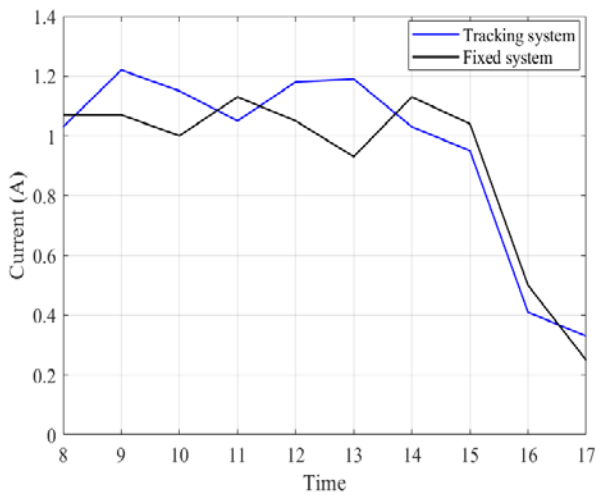

Figure 16. The power generated on the 2nd day

Figure 15. The short-circuit currents on the 2nd day

On the third-day of testing, the open-circuit voltages produced by the fixed system is more stable compared to the voltages resulting from the solar tracking system that slightly decrease after 1 p.m. as presented in Figure 17. This condition happens due to the system's inability to obtain the maximum voltage point.

Nevertheless, the current value increased, particularly after 12:00 p.m. This significant increase in value occurred at 14:00 in the afternoon and then decreased until the end of the test. However, the current value is still greater than the value produced by the fixed system as shown in Figure 18. Meanwhile, the maximum power generated occurs at 2 p.m. after which the power output decreased due to a decrease in solar radiation caused by the presence of clouds. This is shown in Figure 19. The system that employs the tracking concept still generates more power.

Table 4. Test parameter value every hour during the test on third day

| Time	Voltage (V)		Current (A)		Power (W)		Temperature (^{0}C)	Humidity (%)	Irradiance (W/m^2)
	Fixed system	Tracking system	Fixed system	Tracking system	Fixed system	Tracking system			
08.00	20.38	21.31	0.34	0.41	6.93	8.74	28.40	44.00	215.03
09.00	20.58	21.56	0.37	0.45	7.61	9.70	31.70	35.00	426.40
10.00	20.43	20.82	0.54	0.57	9.40	11.87	33.80	16.00	683.95
11.00	20.48	20.68	0.46	0.54	9.42	11.17	36.10	14.00	1007.31
12.00	20.53	20.53	0.46	0.46	9.44	9.44	21.30	20.00	720.22
13.00	20.48	20.53	0.44	0.49	9.01	10.06	34.00	18.00	1146.75
14.00	20.58	19.51	0.39	0.81	8.03	15.80	32.90	32.00	528.71
15.00	20.53	19.99	0.45	0.50	9.24	10.00	31.20	37.00	376.96
16.00	20.48	19.70	0.45	0.40	9.22	7.88	27.20	44.00	239.76
17.00	20.58	19.90	0.30	0.34	6.17	6.76	27.90	40.00	5.16
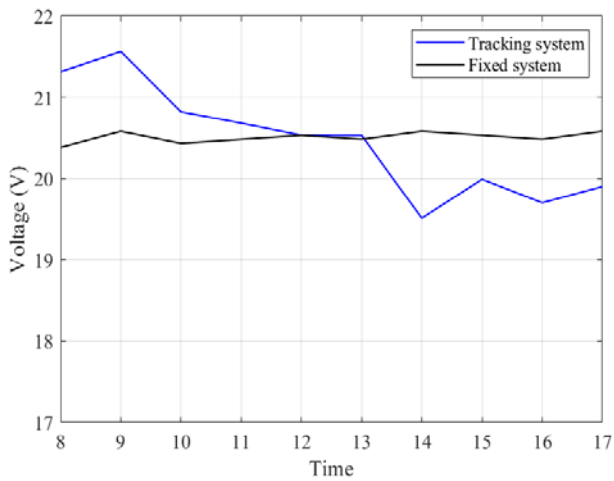
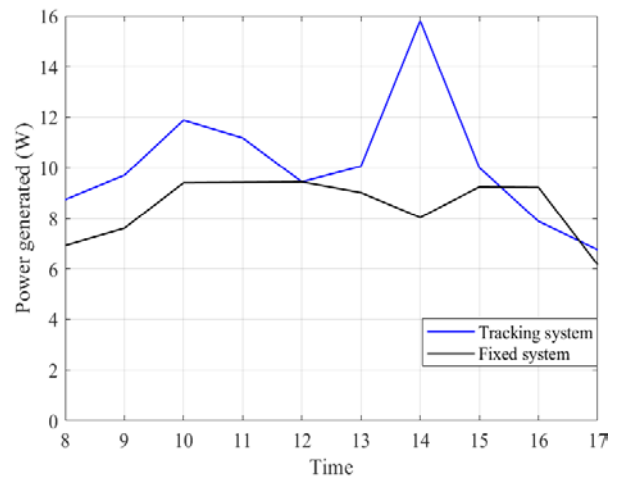*Figure 17. Open-circuit voltages on the 3rd day*

Figure 19. The generated power on the 3rd day
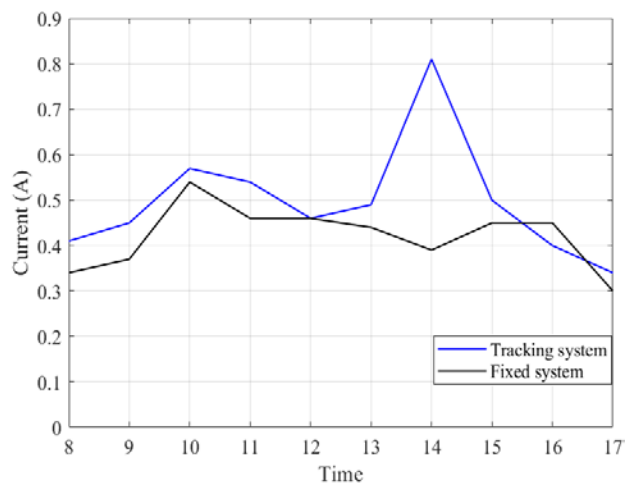

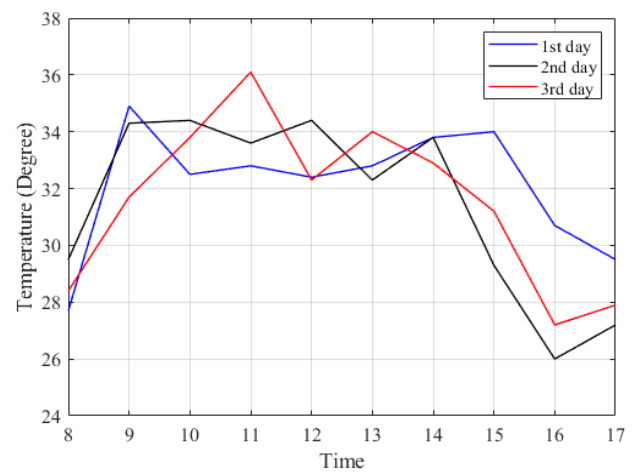*Figure 18. The short-circuit currents on the 3rd day*

Figure 20. The temperature for three days of testing

Figure 20 depicts the variation in temperature over the three days of testing. The temperature increases at the beginning then it becomes more stable between 9:00 and 12:00 p.m., and decrease until the end of the test. On the third day of testing, the difference between morning and evening temperatures is readily apparent. Changes in temperature also result in alterations in humidity levels. The humidity value shows an inverse relationship with temperature, as illustrated in Figure 21. As the temperature decreases, the humidity value increases, and vice versa.

Figure 22 compares the solar irradiance values measured over three days. This value has a substantial effect on the quantity of electricity solar modules produce. The presence of clouds that prevent sunlight from reaching the solar module's surface is the primary cause of the difference in radiation values during the test. On the first day of testing, performance was quite good until 14:00 p.m., after which there is a sharp decline until the test concluded.
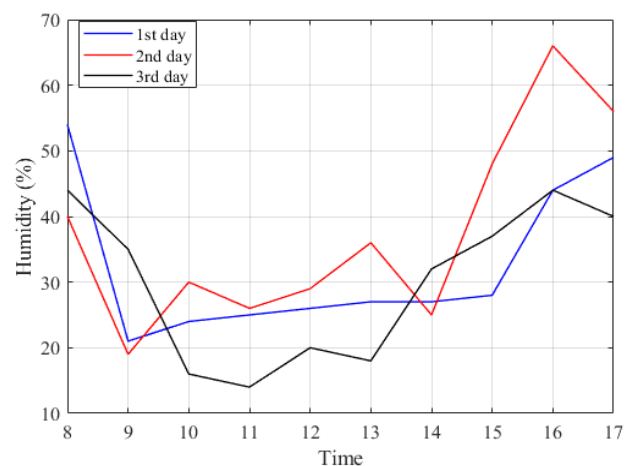

Figure 21. The humidity for three days of testing

The second and third day of testing were inconsistent, particularly the third day. But overall, solar radiation decreases dramatically from midday to the end of the test for three consecutive days.
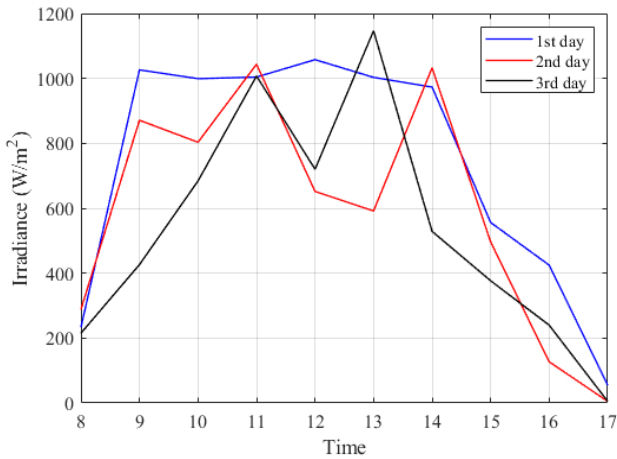
Figure 22. The solar irradiance for three days of testing

During the three tests, the system constructed using the concept of a single-axis solar tracking system performed better than the fixed system. Figure 23 depicts a comparison of the average production of electrical energy during the test, which simultaneously demonstrates that the constructed tracking system can increase the electrical energy production despite employing low-cost components.
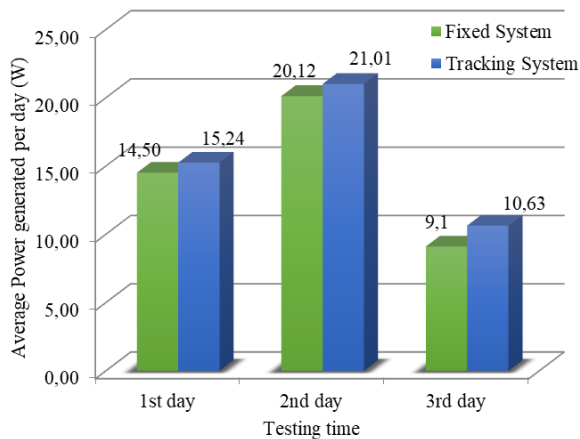

Figure 23. The test's daily average electrical energy

Figure 23 depicts the average amount of energy produced per day during the test. The first day of the test, has mostly clear skies and sunny weather, although there are also quite a few clouds. On the second day of the test, the weather is clear and sunny, whereas on the third day, the sky was overcast and it rained both in the morning and in the evening. According the test results, the solar tracking system is more capable of producing a greater amount of electrical energy than a fixed system. During the three days of testing, the test results demonstrate that the solar tracking system, despite being simple and inexpensive, can increase the production of electrical energy. The greatest improvement, 14.4%, was realized on the third day of testing.

5. Conclusion

The performance of solar modules can be considerably increased by utilizing a dynamic axis solar tracker with IoT-enabled performance monitoring. The research discovered that, when compared to the static axis installation, the solar module positioned on the dynamic axis and powered by a single-axis solar tracker produced more power. Real-time data analysis, remote access, and automatic reporting were made possible by the IoT-enabled performance monitoring system, which can improve solar system performance, efficiency, and maintenance. To improve the productiveness of solar systems, this study illustrates the potential advantages of merging solar tracking technology with IoT-enabled performance monitoring.

References:

[1]. Al-Amayreh, M. I., & Alahmer, A. (2022). On improving the efficiency of hybrid solar lighting and thermal system using dual-axis solar tracking system. *Energy Reports*, 8, 841–847.

[2]. Mehdi, G., Ali, N., Hussain, S., A. Zaidi, A., Shah, A. H., & Azeem, M. M. (2019). Design and fabrication of automatic single axis solar tracker for solar panel. *International Conference on Computing, Mathematics and Engineering Technology-ICoMET 2019*, 1–4.

[3]. Ghassoul, M. (2018). Single axis automatic tracking system based on PILOT scheme to control the solar panel to optimize solar energy extraction. *Energy Reports*, 4, 520–527.

[4]. Dinçer, H., Yüksel, S., Aksoy, T., Hacıoğlu, Ü., Mikhaylov, A., & Pinter, G. (2023). Analysis of solar module alternatives for efficiency-based energy investments with hybrid 2-tuple IVIF modeling. *Energy Reports*, 10, 61–71.

[5]. Munanga, P., Chinguwa, S., & Nyemba, W. R. (2020). Design for manufacture and assembly of an intelligent single axis solar tracking system. *Procedia CIRP*, 91, 571–576.

[6]. Khare, V., Chaturvedi, P., & Mishra, M. (2023). Solar energy system concept change from trending technology: A comprehensive review. *E-Prime - Advances in Electrical Engineering, Electronics and Energy*, 4, 1–20.

[7]. Wang, Y. (2022). Methods for increasing the conversion efficiency of solar cells. *Journal of Physics: Conference Series*, 2221(1), 1–7.

[8]. Parthiban, R., & Ponnambalam, P. (2022). An Enhancement of the Solar Panel Efficiency: A Comprehensive Review. *Frontiers in Energy Research*, *10*, 1–15.

[9]. Lee, J. F., Rahim, N. A., & Al-Turki, Y. A. (2013). Performance of dual-axis solar tracker versus static solar system by segmented clearness index in Malaysia. *International Journal of Photoenergy*, *2013*, 1–13.

[10]. Imthiyas, A., Prakash, S., Vijay, N., Alwin Abraham, A., & Kumar, B. G. (2020). Increasing the efficiency of solar panel by solar tracking system. *IOP Conference Series: Materials Science and Engineering*, *993*(1), 1–7.

[11]. Garg, A., Kumar, K., Kumar, R., & Saini, S. (2015). Solar tracking: an efficient method of improving solar plant efficiency. *International Journal of Electrical and Electronics Engineering*, *7*(1), 199–203.

[12]. Basher, M. M., Aga, H., & Saad Basher, S. (2022). Increasing The Efficiency Of Solar Energy Systems Using The Sun Tracking Method (Design And Implementation). *Webology*, *19*(2), 1–12.

[13]. Yilmaz, S., Riza Ozcalik, H., Dogmus, O., Dincer, F., Akgol, O., & Karaaslan, M. (2015). Design of two axes sun tracking controller with analytically solar radiation calculations. *Renewable and Sustainable Energy Reviews*, *43*, 997–1005.

[14]. Zainal, N. A., Ajisman, & Yusoff, A. R. (2016). Modelling of Photovoltaic Module Using Matlab Simulink. *IOP Conference Series: Materials Science and Engineering*, *114*(1).

[15]. Hafez, A. Z., Yousef, A. M., & Harag, N. M. (2018). Solar tracking systems: Technologies and trackers drive types – A review. *Renewable and Sustainable Energy Reviews*, *91*, 754–782.

[16]. Gutierrez, S., Rodrigo, P. M., Alvarez, J., Acero, A., & Montoya, A. (2020). Development and testing of a single-axis photovoltaic sun tracker through the internet of things. *Energies*, *13*(10).

[17]. Nahar, M. J., Sarkar, M. R., Uddin, M., Hossain, M. F., Rana, M. M., & Tanshena, M. R. (2021). Single Axis Solar Tracker for Maximizing Power Production and Sunlight Overlapping Removal on the Sensors of Tracker. *International Journal of Robotics and Control Systems*, *1*(2), 186–197.

[18]. Jovanovic, V. M., Ayala, O., Seek, M., & Marsillac, S. (2016). Single axis solar tracker actuator location analysis. *Conference Proceedings - IEEE SoutheastCon*, 1–5.

[19]. Kulkarni, A., Kshirsagar, T., Laturia, A., & Ghare, P. H. (2013). An intelligent solar tracker for photovoltaic panels. *Proceedings - 2013 Texas Instruments India Educators' Conference*, 390–393.

[20]. Mallick, T. C., Munna, M. S., Barua, B., & Rahman, K. M. (2014). A design & implementation of a single axis solar tracker with diffuse reflector. *The 9th International Forum on Strategic Technology (IFOST)*, 289–293.

[21]. Afanasyeva, S., Bogdanov, D., & Breyer, C. (2018). Relevance of PV with single-axis tracking for energy scenarios. *Solar Energy*, *173*, 173–191.

[22]. Duffie, J. A., Beckman, W. A., & Blair, N. (2020). *Solar engineering of thermal processes, photovoltaics and wind*. John Wiley & Sons.